LIGHT EMISSION IN THE VACUUM ULTRAVIOLET THROUGH ELECTRON COLLISION EXCITATION IN GASES

Part A: Investigations in Oxygen

W. Sroka

Translation of: "Lichtemission im Vakuum-ultraviolet durch Elektronenstobrarregung in Gasen Teil: A: Untersuchungen in Sauer-stoff", Zeitschrift für Naturforschung, Vol. 23, 1968, pp. 2004-2013.

NATIONAL AERONAUTICS AND SPACE ADMINISTRATION
WASHINGTON, D.C. 20546 APRIL 1973

STANDARD TITLE PAGE

1. Report No.	2. Government Accession No.	3. Recipient's Catalog No.
NASA TT F-14,728		

4. Title and Subtitle
LIGHT EMISSION IN THE VACUUM ULTRAVIOLET THROUGH ELECTRON COLLISION EXCITATION IN GASES. A: INVESTIGATIONS IN OXYGEN

5. Report Date
April 1973

6. Performing Organization Code

7. Author(s)
W. Sroka

8. Performing Organization Report No.

10. Work Unit No.

11. Contract or Grant No.
NASW-2482

9. Performing Organization Name and Address
Linguistic Systems, Inc.
116 Austin Street
Cambridge, Mass. 02139

13. Type of Report and Period Covered
Translation

12. Sponsoring Agency Name and Address
NATIONAL AERONAUTICS AND SPACE ADMINISTRATION
WASHINGTON, D.C. 20546

14. Sponsoring Agency Code

15. Supplementary Notes
Translation of: "Lichtemission im Vakuumultraviolet durch Elektronenstobrarregung in Gasen Teil: A: Untersuchungen in Sauerstoff", Zeitschrift für Naturforschung, Vol. 23, 1968, pp. 2004-2013.

16. Abstract

A nearly monochromatic electron beam of low energy (0-200 eV) interacts with molecules of a gas (O_2, N_2, etc). The radiation emitted in this collision process is observed with a vacuum-monochromator. The registered wave-length can be attributed to known transitions. The excitation-functions and the appearance potentials of these processes are measured. It is found that the electrons dissociate the molecules in a single collision into excited atoms or ions which emit a radiation in the vacuum-ultraviolet. Furthermore it is shown that the above mentioned processes also appear in low-current corona-discharges and in non-self-sustaining discharges in the homogeneous electric field. The origin of the so-called gas-ionizing radiation is found to be a dissociation process combined with an excitation of the dissociation products.

17. Key Words (Selected by Author(s))	18. Distribution Statement
	UNCLASSIFIED - UNLIMITED

19. Security Classif. (of this report)	20. Security Classif. (of this page)	21. No. of Pages	22. Price
UNCLASSIFIED	UNCLASSIFIED	28	4.25

LIGHT EMISSION IN THE VACUUM ULTRAVIOLET THROUGH ELECTRON COLLISION EXCITATION IN GASES[†]

Part A: Investigations in Oxygen

W. Sroka[‡]

1.1 Introduction

In the present paper, excitation processes of gases by slow /2004 electrons (0-200 eV) are investigated, which lead to emission of radiation in the vacuum ultraviolet. In these processes the gas molecules (O_2, N_2, CO, etc.) are dissociated in a simple collision into excited fragments—atoms or ions. These subsequently emit very short-wave light, for example:

$$X_2 + e^- = X + X^* + e^-$$
$$X^* \rightarrow X + h\cdot\nu$$

or

$$X_2 + e^- = X + X^{+*} + 2e^-$$
$$X^{+*} \rightarrow X^+ + h\cdot\nu .$$

The absolute values of the excitation functions lie between 10^{-17} and 10^{-19} cm^2. A minimum energy is necessary for the occurrence of dissociative excitation processes. It is equal to the sum of the excitation, dissociation, and, if circumstances require, of the ionization energy. From this threshold potential one can frequently conclude to the energy state of the second dissociation product. A current discussion of these results can be found in [1].

[†]Abbreviated version of a thesis, University of Hamburg, 1968.

[‡]Institute for Applied Physics of the University of Hamburg.

(Z. Naturforsch. 23a, 2004-2013, 1968; received Sept. 9, 1968.

*Numbers in righthand margin indicated pagination of foreign text.

It can be shown that the dissociative excitation processes also occur in non-independent discharges in a homogeneous electric field and in weak current corona discharges. In these processes, such lines, among others, are excited whose wavelength is shorter than the ionization wavelength of the initial molecules. In a /2005 series of previous papers [2-5], this so-called gas ionizing radiation has been treated. The mechanism for generating this radiation can only be understood as a dissociative excitation process [1]. In the papers mentioned, the various parts of the gas ionizing radiation were characterized by their respective absorption coefficients. These components can now be associated with their corresponding wavelengths. Furthermore, the associated transitions can be ordered into well-known level schemes.

The measurement program includes the determination of wavelengths of the radiation components which occur during collision processes as well as their excitation functions. In reference to the investigation of the gas ionizing radiation, the spectra on the above-mentioned discharge types as well as the absorption coefficients on individual lines must be measured.

1.2 Measuring Principle

To measure the excitation function, an electron beam of variable energy is directed into a collision cell filled with the gas to be investigated. The pressure in the cell is maintained sufficiently low ($p < 10^{-3}$ torr) that multiple collisions are excluded. The luminous gas column at the locality of the electron beam is investigated with a vacuum monochromator. An open multiplier serves as detector. A recorder registers the intensity directly for each of the respective radiation components, as a function of the colliding electron energy. On the other hand, the spectral intensity distribution of the radiation at constant electron energy can be determined. The setting of the monochrometer wavelength is achieved

by rotation of a screen which is coupled with the paper advance of the recorder.

The collision cell at the entrance of the spectrograph can be replaced by a collision chamber. In this chamber can be arranged optionally a weak current corona discharge or a non-independent discharge in a homogeneous electric field. These resemble those used in [3] and [4]. With the apparatus modified in this fashion the spectrum in each of the respective discharges can be measured. Furthermore, the absorption coefficients of the individual radiation components can be determined. For this purpose the pressure in the spectrograph is varied at constant discharge conditions in the light source. From the behavior of the intensity as a function of pressure in the absorption chamber, the absorption coefficient can be determined.

1.3 The Collision Apparatus and the Vacuum Monochrometer

Figure 1 shows a sketch of the collision apparatus. The electron beam is generated in a Pierce gun, and has a cross-section 0.04 cm x 1.5 cm. An indirectly heated nickel sinter cathode [6] is used, which is relatively insensitive with respect to oxygen. Beam limiting occurs at electrode E_4. The voltage at electrode E_5 lies near the cathode potential, so that the secondary electrons generated at the preceding electrodes can be kept away from the collision chamber. The diaphragm cross-section of the remaining electrodes is greater than that of E_4. The entrance and exit the electron beam into or out of the collision cell is effected through pressure steps. In order to hold back the secondary electrons generated at the receiver, the electrode E_9 also lies near the cathode potential. The voltages on E_6 and E_8 are arranged so that the current at the receiver (maximum 150 μA) remains constant upon variation of the collision cell voltage. The beam is collimated along its length by a homogeneous magnetic field (100-400

Gauss). During operation, the electrode system is maintained at a temperature of about 250° C, in order to reduce contamination of the diaphragm.

Figure 2 shows a sketch of the collision apparatus in cross-section. The radiation—generated at the place of the electron beam—goes through a pressure stage into the grating of the monochromator (type Seya-Namioka). The grating is made of platinum and has 1200 lines/mm. At the exit of the monochromator a slit width of 0.4 mm has been chosen. The multiplier signal (Bendix M 306) is placed on the y-coordinate of a two-channel recorder, via an amplifier and a coupled rate meter. The x-channel shows the voltage of the collision cell. The beginning of the ion stream can be measured with a probe and with a subsequent direct current amplifier.

The wavelength resolution of the collision apparatus is only about 12 Å, since the luminous gas column is directly imaged on the exit slit (without entrance slit), because of its low intensity.

Calibration of the energy scale of the colliding electrons is achieved by measuring the threshold potential of the He resonance line ($2p\ ^1P \rightarrow 1s\ ^1S$) at 584 Å, which lies at 21.2 eV. About 10-20% He is added to the gas under investigation. The process is explained, by way of example, in Fig. 3 for the oxygen line (λ = 833 Å). At first the excitation function of the He line is measured; then the oxygen line. As a control the excitation function of the He line is then checked again. The threshold potential of the He line marks the energy value 21.2 eV. The energy scale can also be calibrated by measurement of the ion stream threshold (see Fig. 2)—even though with less accuracy. The accuracy of /2007 the measurement of the threshold potential comes at most to about ±0.8 eV—according to the intensity of the line under consideration.

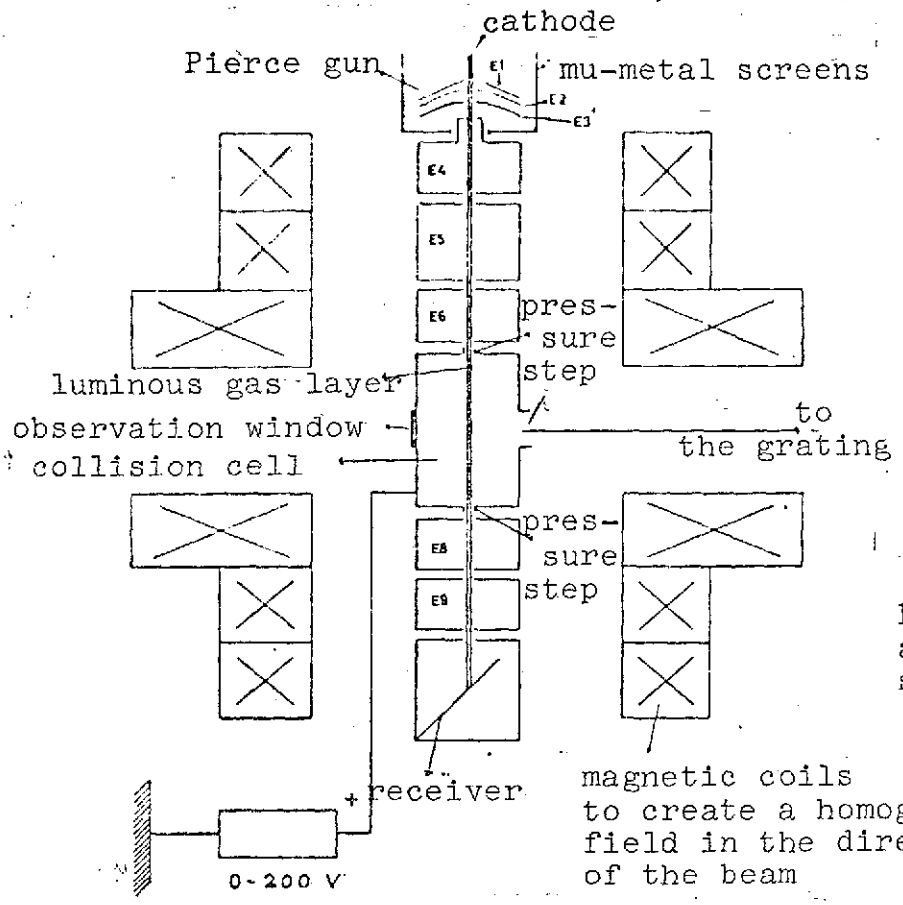

Fig. 1. The collision apparatus, lengthwise section.

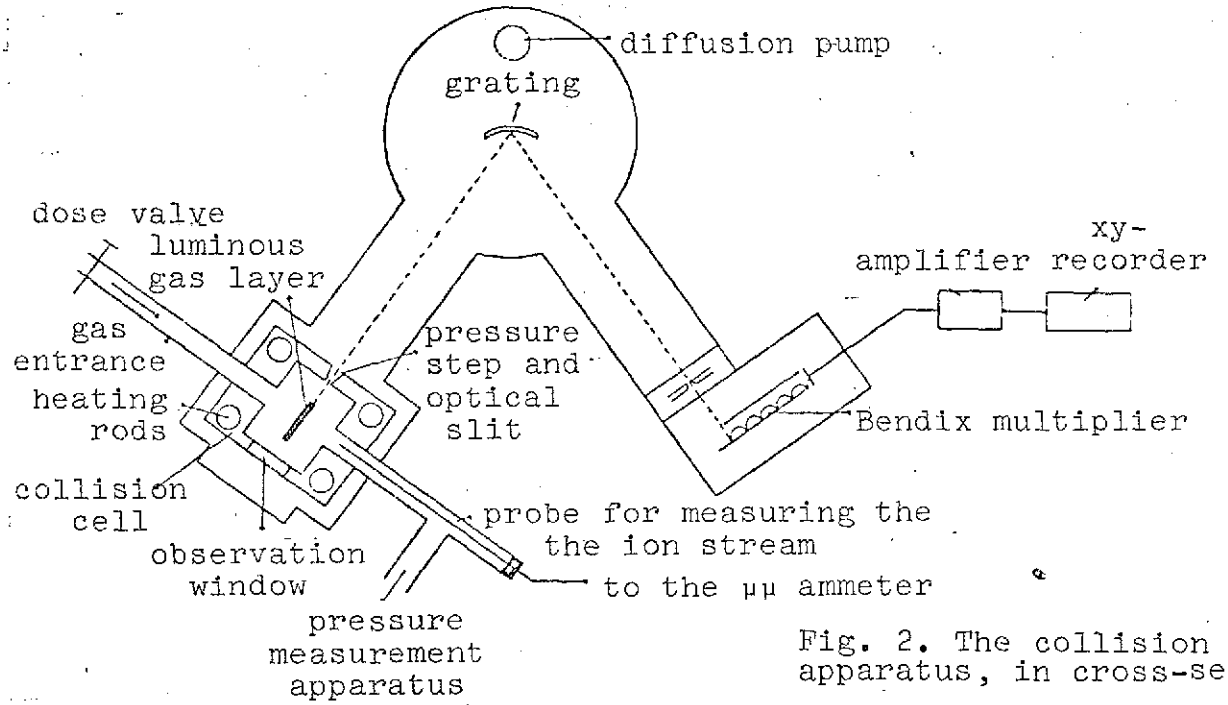

Fig. 2. The collision apparatus, in cross-section.

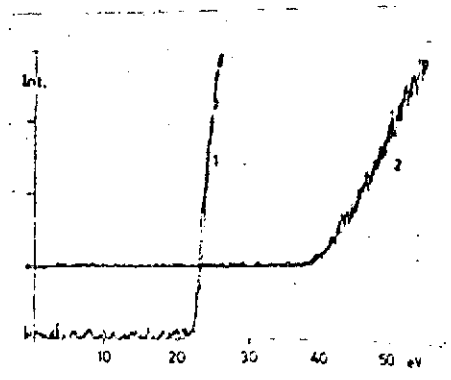

Fig. 3. The curves 1 and 2 show the excitation function of an He line (λ=584 Å) and an oxygen line (λ=833 Å). The excitation function of the He line was traversed twice for control purposes. The threshold voltage of the He line lies at 2.2 eV. The energy scale is calibrated by this value. The measurement yields a threshold potential for the OH line of 37.5 eV. It must be noted here that the excitation function begins with a bend.

1.4 Determination of the Absolute Values of the Excitation Functions

To determine the absolute values of the excitation functions, helium gas is added to the sample gas. The intensity of the respective line is then compared with that of a helium line (584 Å) under similar excitation conditions. The absolute value of the excitation function of the helium line can be determined with the help of data available in the literature [7,8]. The wavelength dependence of the grating reflection [9,10] and the quantum yield of the multiplier cathode (tungsten) must be considered as corrections. The reflection capability of the grating and the quantum yield of the photocathode can, under some circumstances, be influenced by layers of foreign matter. It is further possible that the collision cell has a somewhat different gas mixture than the supply container. Calibration of the intensity scale can therefore only give a preliminary approximation for the absolute value of the excitation function. Errors in the intensity ratios of neighboring lines (wavelength separation $\Delta\lambda < 200$ Å) will be small (below 10%). But larger errors can appear in the absolute values and in the intensity ratios of lines more distant from one another.

1.5 Measurement of Spectra from Corona Discharges

To determine the spectra from corona discharges, a discharge region is installed at the entrance of the spectrograph. It consists of a cylindrical pipe in whose middle a corona discharge takes

place at a coaxial inner conductor (50-300 μ diameter). The current intensity can be chosen between 0.5 μA and 30 μA, according to the pressure domain. The current reading refers to that part of the discharge path from which photons reach the grating. The radiation reaches the monochromator through a slit—which simultaneously serves as a pressure step. Positive as well as negative polarity of the inner conductor was used in this process.

The pressure in the discharge chamber can come up to 15 torr, according to the slit width (70-300 μ), without the monochromator pressure rising above 10^{-3} torr. Gas supply in the discharge chamber is through a needle valve. To avoid contamination effects, the inner conductor is heated to low red heat during operation.

The wavelength scale is calibrated by measurement of known lines of helium or argon. In this arrangement a measurement of the wavelength is achieved of about 1-2 Å. Resolving power is here about 5-8 Å. Both magnitudes are determined by the slit opening (exit slit width equal to entrance slit width). The choice of slit width again depends on the intensity of radiation.

1.6 Measurement of the Absoprtion Coefficient

To determine the absorption coefficient of individual radiation components, the discharge parameters (pressure, X/p, and current) are held constant, and the pressure in the monochromator is varied. For this purpose the pumping effect of the pump is throttled and besides the gas is emitted into the monochromator through a second needle valve (flow-through process). The monochromator pressure (10^{-3} to 10^{-1} torr) is measured with McLeod manometer (measurement accuracy about 5%). Furthermore, during this measurement the open multiplier must be replaced by a closed one (type EMI 9502 S), because of the high manochromator pressure. The front side of this device has a sodium salicylate layer as radiation convertor. To

reduce dark current, the thermally isolated multiplier is kept at a temperature of about -60° C.

1.7 Measuement of the Spectrum of a Non-Independent Discharge in a Homogeneous Electric Field

To investigate the emission of radiation of a non-independent discharge in a homogeneous electric field, the discharge region (90° Rogowski profile; plate separation 3 cm maximum) is so arranged at the entrance of the spectrograph that the entrance slit lies at the anode.

The inner part of the cathode consists of a quartz plate on which a Pd-film of about 300 Å thickness is sputtered [11]. Primary electrons are ejected from the cathode by means of a flash-lamp, and an electrode avalanche forms which runs to the anode. The anode emits very short-wave radiation. Since the intensity in this experiment (maximum 3 flash impulses) is of the same order of magnitude as the dark current of the multiplier, a linear gate circuit is arranged between the secondary electromultiplier and the counting device. The gate is opened by a trigger impulse on the flash lamp, for the time that photons are emitted from the discharge line.

2.1 Measurement Results from the Collision Experiment /2008

Radiation in the extreme ultraviolet (λ < 1100 Å) arises from the interaction of slow electrons (E_{kin} < 200 eV) with oxygen molecules. Fig. 4a shows a spectrum taken with the apparatus explained in Section 1.3. The energy of the colliding electrons was 60 eV. The wavelength of individual components are tabulated in numerical order in Table 1. Fig. 5 shows the excitation sections of the lines which have been measured with the arrangement described in Section 1.3. The threshold potentials and the approximations determined in accord with Section 1.4 for the absolute values of the excitation

functions at 100 eV are likewise found in Table 1. The excitation functions of all the lines could not be determined because of low intensity.

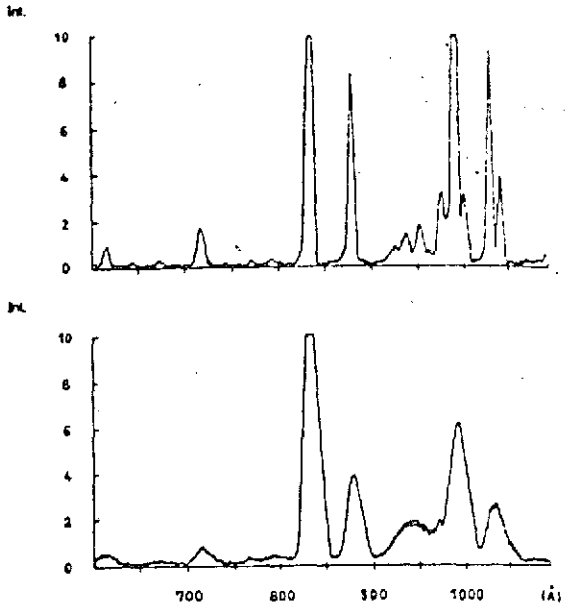

Fig. 4a (below). Spectrum of oxygen excited by approximately monoenergetic electrons with energy 60 eV.

Fig. 4b (top). Spectrum of a corona discharge, likewise in oxygen. Resolving power is less in Fig. 4a than in 4b, because of intensity reasons.

2.2 Discussion of the Excitation Process

The lines appearing in the spectra of Fig. 4a can be unambiguously identified as the O I- and O II-lines, by comparison with spectroscopic data [12-16]. Molecular radiation does not appear in oxygen in this wavelength region. This is furthermore confirmed by the relatively high threshold potential. Table 1 shows the associated transitions. Because of low pressure in the collision chamber ($p < 10^{-3}$ torr), the excitation of this atomic or ionic radiation can only result in a process in which an electron dissociates the O_2 molecule into excited fragments in a single collision.

One of the fragments—an atom or ion—is excited and emits light in the region of the vacuum ulraviolet.

The excitation functions (Fig. 5) not only represent the interaction cross-section for direct excitation of these levels, from which emission occurs, but can implicitly contain excitation cross-sections of higher levels which contribute to the population of the observed level—according to the respective transition probability.

The threshold of the excitation function is linear (Fig. 5); only the line at 833 Å shows a positively curved behavior immediately at the threshold value.

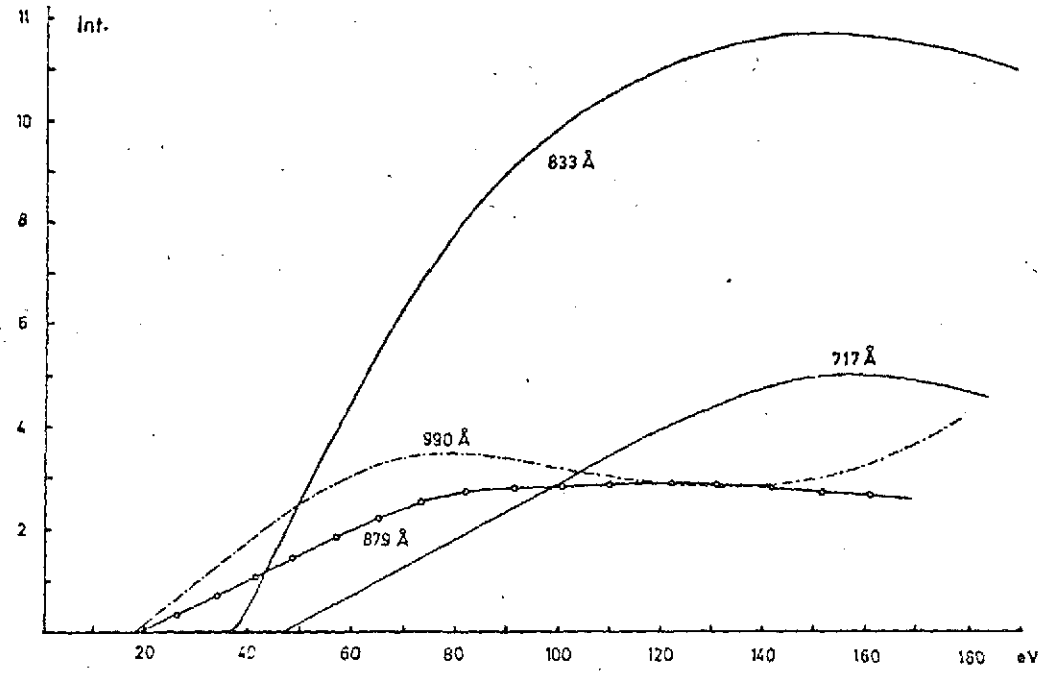

Fig. 5. Excitation functions in oxygen. The ordinate is divided into arbitrary units. Absolute values for the excitation function can be taken from Table 1.

It is remarkable that the excitation function of the component with λ = 990 Å shows a new rise at higher energies. In the neighborhood of λ = 990 Å, there are a number of O I-lines, which cannot

be completely resolved by the monochromator. It is possible that the rise can be based on the increased excitation of one of the lines at higher energies. It is also conceivable that the λ = 990 Å line results from several competing dissociating processes, one of which only becomes effective at high energies.

The minimum energy necessary for the excitation of one O I-line equals the sum of the excitation and dissociation energy (5.1 eV). For the excitation of the O II-line ionization energy must also be included (13.6 eV). In view of the measured threshold potentials /2009 and under consideration of the uncertainty in measurement for the voltages used (±0.8 eV), it can therefore be asserted that the second dissociation product for lines number 5 (879 Å), 9 (990 Å), and 11 (1028 Å) is an oxygen atom in the ground state ($2p^4\ ^3P$). Thus, for instance, the following dissociative excitation process results for line 9:

$$O_2(X\ ^3\Sigma_g^-) + e^-(E_{Kin} > 18\ eV) = O(2p\ ^3P) + O(3s\ ^3D) + e^-$$

The transition $O(3s\ ^3D) \rightarrow O(2p\ ^3P)$ gives radiation with λ = 990 Å (12.5 eV).

In the region from 17 eV to 20 eV—that is, where the threshold potentials lie—the absorption spectrum of O_2 has strong structure. The absorption lines have not yet been classified [17]. Likewise the electron emission spectrum of O_2 has structure [18]. It is therefore conceivable that the excitation happens through an intermediate step, i.e., a highly excited molecular state is formed first, which then dissociates into excited atoms. Except for the total angular momentum, the quantum mechanical states of the dissociation products are indeed known, but no unambiguous conclusions can be drawn from this with respect to the intermediate state, if it is formed at all [19].

For line 4 (833 Å), the measured threshold potential lies about 4.1 eV above the calculated minimum value. The excess energy can be given off wholely or in part in the form of kinetic energy of the dissociation partner. In [20] it is shown that in dissociation processes of O_2, fragments with kinetic energies up to 10 eV and more can appear. Further, it would be energetically possible that the second dissociation product is an O atom in the $2p\ ^1S$- or $2p\ ^1D$-state (4.2 eV or 1.9 eV above the ground state). In a Grotrian diagram of O II [21] no cascade transition into the $2p^4\ ^4P$-level of O II are shown. Therefore the possibility of a primary /2010 excitation of O II levels (maximum 4.1 eV above $2p^4\ ^4P$) and following cascade processes there into the $2p^4\ ^4P$-state can here be excluded.

The excess energy of the radiation component 3 (717 Å) comes to about 8.3 eV. Here the second dissociation product can be an excited O atom. Further, the higher excited O II ion can be first formed, which populates the $2p'\ ^2D$-level trough cascade transitions. Finally the excess energy can be given at kinetic energy to the dissociation partner, if in the primary process an electron transition takes place into the strongly repelling potential curve of O_2^+.

3.1 Results Concerning Gas Ionizing Radiation from Previous Shower Experiments

Gas ionizing radiation is characterized by its ability to ionize the original gas; the wavelength is therefore shorter than the ionization wavelength (for O_2 this is λ_1 = 1027 Å). In a series of researches (see [2-5] and the literature cited there), it has been shown that gas ionizing radiation does exist in oxygen. This radiation appears in corona discharges as well as in non-independent discharges in homogeneous electric fields. Three radiation components have been demonstrated with absorption coefficients μ_1 = 38 cm,

[sic], $\mu_2 = 250\ cm^{-1}$, $\mu_3 = 500\ cm^{-1}$. For the first two components the number of photons per ionization event (ω/α) was measured in [3] as a function of X/p (field strength/pressure); besides the extinction pressure was determined. It could be shown that the intensity of gas ionizing radiation was in all cases strictly proportional to the discharge current density. The absorption coefficient $\mu_1 = 38\ cm^{-1}$ proved to be pressure independent. But the origin of the gas ionizing radiation remains unexplained, since nothing could be said concerning its spectral intensity distribution.

3.2 The Excitation Mechanism for Gas Ionizing Radiation

As Fig. 4b shows, a corona discharge (shower experiment, compare 1.5) has the same radiation component as a collision experiment (Fig. 4a). The wavelength of the lines can be measured here with more favorable resolving power and with greater accuracy because of the increased intensity. With the aid of these measurements, Table 1 was completed. The spectrum shown in Fig. 4b was taken at an operating pressure of p = 0.6 torr. When pressure is reduced further, the corona discharge becomes unstable. The current intensity here came to 29 μA. But the intense radiation components can still be observed at currents below 1 μA. If one works at higher pressures, then only the weakly absorbed components reach the entrance slit of the monochromator. Besides the pressure rise influences the intensity of the discharge through collision quenching and through the altered value of X/p.

Continuation of the spectrum towards longer wavelengths—whose reproduction has here been dispensed with—shows further O I-lines. These radiation components are also given in Table 1.

Sections of the spectrum of an oxygen discharge in a homogeneous electric field are given in Fig. 6. It was taken with the apparatus described in Section 1.7, with X/p ≈ 250 volt/torr·cm. Because of low intensity—maximum 3 impulses per flash at the multiplier

exit—the spectrum was traversed very slowly with a large integration time constant. The lines in Fig. 6, therefore, can be represented only singly.

Investigations show that a non-independent discharge in a homogeneous field emits the same radiation components as a corona discharge. According to 2.2, the lines can be excited in a one-step dissociation process. Since, according to 3.1, the intensity for shower experiments is strictly linear in proportion to the discharge current, the excitation here must also be in a single step, namely through the dissociation process treated in Section 2. As the spectra show, such lines are emitted here whose wavelength is shorter than the ionization wavelength of the oxygen molecule. The origin of the gas ionizing radiation can consequently be understood in atom-physical terms as a dissociative excitation process.

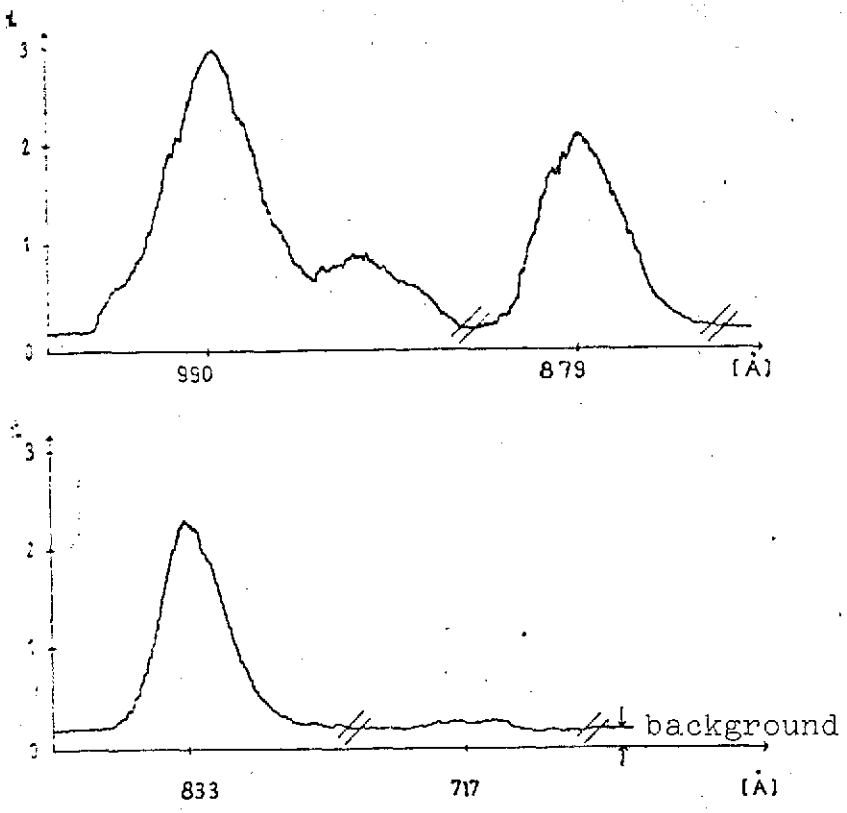

Fig. 6. Sections of a spectrum of a non-independent discharge in a homogeneous electric field. Because of the large integration time constant, the lines were traversed singly from lower to greater wavelengths. The side maximum at the right of the radiation component at λ=990 Å represents line 10 (999.5 Å). The line at 717 Å expresses itself only as a weak rise in the background.

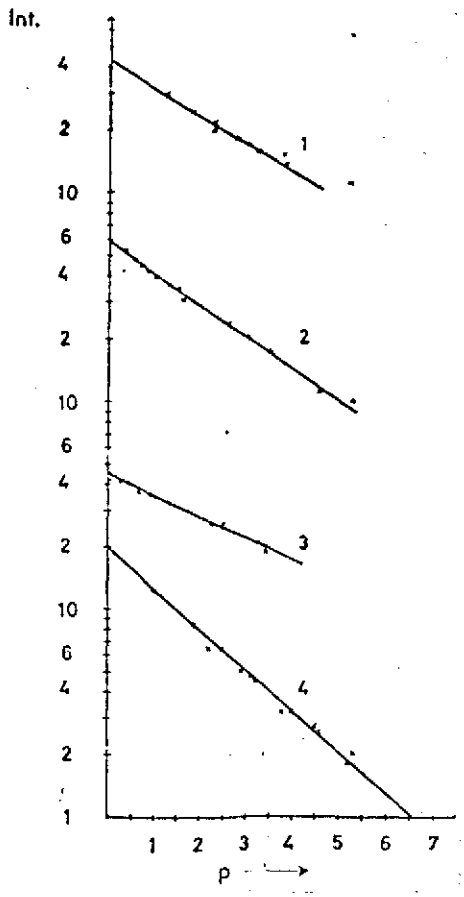

Fig. 7. The intensity of several oxygen lines is plotted semi-logarithmically against the pressure in the absorption chamber. 1) λ=999.5 Å; 2) λ=833 Å; 3) λ= = 880 Å; 4) λ=990 Å. As abscissa unit the value 10^{-1} torr was chosen for the straight lines 1 and 4, and the value 10^{-2} torr for the straight lines 2 and 3.

3.3 Remarks Concerning the Investigations in a Homogeneous Field /2011

Fig. 6 shows that the signal-to-background ratio is sufficient to investigate the intensity of individual lines as a function of discharge parameters. Since the absorption coefficients and the excitation functions are known, it would be possible to draw conclusions from this concerning the extinction pressure and the energy distribution of the fast electrons.

3.4 The Absorption Coefficients of the Gas Ionizing Radiation and Comparison with Prior Investigations

The individual components of gas ionizing radiation have been distinguished [3] and [4] through their absorption coefficients.

In this research the wavelength of gas ionizing radiation was determined. If the absorption coefficients of individual lines are also measured, then the radiation components investigated in [3] and [4] can be assigned appropriate wavelengths. The absorptions in [3] concerning the extinction pressure and the behavior of ω/α as a function of X/p can be connected with the results of this research.

The absorption coefficients of the gas ionizing radiation in O_2 are determined in the procedure according to Section 1.6. As an example, Fig. 7 shows the intensity of four lines, plotted semilogarithmically against the pressure in the receiving apparatus. In this representation, the intensity falls linearly with pressure. /201
For every radiation component several such straight lines were measured. From the measured slopes, the absorption coefficient μ can be determined. The values so obtained are entered into Table 1. In the evaluation, the multiplier background was taken into consideration. The error of measurement of the absorption coefficients is around 8-10%.

The ionization wavelength of O_2 lies at 1027 Å. Therefore, line 12 at 1041 Å (μ = 21 cm^{-1}) cannot ionize the O_2 molecule. The ionization effect of line 11 at 1027 Å (μ = 35 cm^{-1}) will be small.

The radiation component chracterized by μ = 38 cm^{-1} in [3] and [4] can be assigned to the lines number 9 and 10 at 990.6 Å (μ = = 41 cm^{-1}) and 999.5 Å (μ = 28 cm^{-1}). The influence of line 9 predominates, since its intensity is substantially greater than that of line 10 (compare Fig. 4b). According to [3], the line 9 can be assigned the extinction pressure of 2.5 torr and the ω/α-value of the radiation component characterized there by μ = 38 cm^{-1}.

In the component with μ = 250 cm^{-1} from [3], the lines 4 at 833 Å (μ = 310 cm^{-1}), 5 at 879 Å (μ = 270 cm^{-1}), and 8 at 974 Å (μ = 170 cm^{-1}) are all contained. The overlap of the radiation

Table 1. Results of investigations in oxygen. The radiation components are numbered continuously. The table uses the published values for the O I- and II-lines which lie closest to the wavelength measured here.

Running no. of the line	1	2	3	4	5	6	7	8	9	10	11	12	13	14	15
measured wavelengh Å	536,8	615,6	717,3	833	879	936,8	951,8	974,2	990,6	999,5	1027,8	1041	1152,5	1217,5	1302,5
published values of Å	537,8	616,4	718,5	833,3	878,9 879,1	936,6 937,8	950,7 950,9	973,9	990,8 990,2	999,5	1027,4 1028,2	1040,9 1039,2	1152,1	1217,6	1302,2
classification of the transition	$2p'\ ^2P$ $2p\ ^2D$ O II	$3s\ ^2P$ $2p\ ^2D$ O II	$2p'\ ^2D$ $2p^3\ ^2D$ O II	$2p^4\ ^4P$ $2p^3\ ^4S$ O II	$3s\ ^3P$ $2p\ ^3P$ O I	$6d\ ^3D$ $2p\ ^3P$ O I	$5d\ ^3D$ $2p\ ^3P$ O I	$4d\ ^3D$ $2p\ ^3P$ O I	$3S\ ^3D$ $2p\ ^3P$ O I	$3s\ ^1P$ $2p\ ^1D$ O I	$3d\ ^3D$ $2p\ ^3P$ O I	$4s\ ^3S$ $2p\ ^3P$ O I	$3s\ ^1D$ $2p\ ^1D$ O I	$3s''\ ^1P$ $2p^4\ ^1S$ O I	$3s\ ^3S$ $2p^4\ ^3P$ O I
threshold potential, eV			47,6	37,7	19,3				18,0		18,1				
calculated min. energy eV			39,3	33,6	19,2				17,6		17,2			19,5	14,6
absolute value of the excitation function at 100 eV $\sigma \cdot 10^{-18}$ cm^2			2	7,6	2,4				3,7						
state of the 2nd dissociation product			excited O I and/or kinetic energy	metastable O I, O($2p\ ^3P$) and/or kinetic energy					O($2p\ ^3P$)		O($2p\ ^3P$)				
absorption coefficient μ	520		500	310	270			170	41	28	35	21			

components numbers 4, 5, and 8 is described through the extinction pressure 0.5 torr and the ω/α-value of the component characterized in [2] by $\mu = 250\ cm^{-1}$.

The strongly absorbed radiation component with $\mu = 550\ cm^{-1}$ (according to [3] and [4]) comes from the components 1 and 3 at 536.8 Å ($\mu = 520\ cm^{-1}$) and 717.3 Å ($\mu = 500\ cm^{-1}$). The line number 2 at 615.2 Å has low intensity, and besides is strongly absorbed (μ is possibly greater than $1000\ cm^{-1}$).

Finally, it should be said that the above results concerning vacuum ultraviolet emission of gases in electron showers agree well with prior results concerning gas ionizing radiation in corona discharges and in non-independent discharges in homogeneous electric fields. They have received a satisfactory explanation through the results of beam experiments reported here.

I express my hearty thanks to Professor Dr. H. Raether for posing the thesis problem and for his constant encouragement of the work. My thanks also go to Dr. W. Legler and Dr. T. H. Teich for many valuable discussions, and to Mr. H. Hertz, candidate in physics, for his collaboration in the investigations in the homogeneous electric field. The work was financially supported by the German Research Association.

REFERENCES

1. Sroka, W., Physics Letters 25 A, 770, 1967.

2. Raether, H., Z. Physick 110, 611, 1938, and Electron Avalanches and Breakdown in Gases, Butterworths, London, 1964.

3. Teich, T. H., Z. Physik 199, 378, 1967.

4. Przybylski, A., Z. Physik, 151, 264, 1958.

5. Przybylski, A., Z. Naturforsch. 16a, 703, 1961; and Z. Physik 168, 504, 1962.

6. Lynch, R. T. and N. B. Hanny, J. Appl. Phys. 24, 1335, 1953.

7. Jobe, J. D. and R. M. St. John, Phys. Rev. 164, 117, 1967.

8. Gabriel, A. H. and D. W. O. Heddle, Proc. Roy. Soc. London, 258 A, 124, 1960.

9. Samson, J. R., J. Opt. Soc. Am. 52, 525, 1962.

10. Madden, R. P. and L. R. Canfield, J. Opt. Soc. Am. 51, 833, 1961.

11. Moruzzi, J. L., Rev. Sci. Instrum. 38, 1284, 1967.

12. Kelly, R. L., A Table of Emission Lines in the Vacuum Ultraviolet for all Elements, Stanford Research Institute, Menlo Park, Calif.

13. Frerichs, R., Phys. Rev. 36, 399, 1930.

14. Moore, C., Atomic Energy Levels, Vol. 1, Circular of the National Bureau of Standards 467, Washington.

15. Edlen, B., Nova Acta Reg. Soc. Sc. Upsala, Ser. 4, Vol. 9, No. 6.

16. White, H. E., Introduction to Atomic Spectra, McGraw-Hill, New York, 1934.

17. Gilmore, F. R., J. Quant. Spectr. Rad. Transf. 5, 369, 1965.

18. Lassettre, E. N., S. M. Silvermann, and M. E. Krasnow, J. Chem. Phys. 40, 1261, 1965.

19. Herzberg, G., Molecular Spectra and Molecular Structure, D. van Nostrand Company, New York, 1950.

20. Rapp, D., P. Englander-Golden, and D. D. Briglia, J. Chem. Phys. 42, 4081, 1965.

21. P. W. Merril Carnegie Institution of Washington, Publication 610.